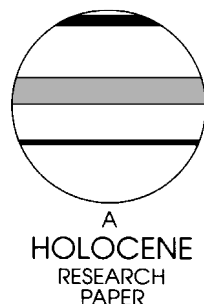


Palynological and AVHRR observations of modern vegetational gradients in eastern North America

John W. Williams^{1*} and Stephen T. Jackson²

(¹National Center for Ecological Analysis and Synthesis, University of California – Santa Barbara, Santa Barbara, CA 93101, USA; ²Department of Botany, University of Wyoming, Laramie, WY 82071, USA)

Received 12 November 2001; revised manuscript accepted 5 June 2002



Abstract: Both fossil pollen records and satellite-based instruments are remote sensors of Earth's vegetation with complementary properties. Satellites supply spatially continuous and highly resolved images for the past several decades, whereas pollen records include local and regional signals of vegetation composition, spanning millennia. Together, pollen and satellite-based observations measure vegetation change across a broad range of temporal scales. Here, we compare pollen percentages of needleleaved and broadleaved plant taxa to AVHRR estimates of percent tree cover, for two regions in eastern North America with well-defined physiognomic gradients. The linear fit between the pollen percentages and percent tree cover is strongest for search window half-widths of 25–75 km and unweighted or inverse-distance weightings, consistent with previous taxon-based studies of regional pollen source area and transport. Variance not explained by the linear model arises primarily from differential properties of the AVHRR and pollen sensors, particularly site-specific variability in the pollen data and intertaxonomic differences in pollen representation. These sources of variance can be minimized by regionally smoothing the pollen data and multivariate analogue approaches. A strong fit between observed tree-cover percentages and best-analogue estimates ($r^2 = 0.70$ to 0.78) suggests that analogue-based methods can be applied to infer past tree-cover proportions from fossil pollen records. Linking pollen and AVHRR observations in this manner effectively extrapolates satellite-derived variables beyond the few decades of direct observation, enabling study of longer-term variations in land cover and impacts upon climate and the terrestrial carbon cycle.

Key words: AVHRR, land cover, plant life forms, pollen analysis, modern analogue technique, remote sensing, vegetation.

Introduction

The advent of satellite-based remote sensing of the Earth's surface has revolutionized global change studies (Roughgarden *et al.*, 1991), but the utility of remotely sensed data is critically limited by their short temporal extent. Remote sensing enables the synoptic imaging of the earth's surface at low cost, with a high spatial precision, and at intraannual temporal resolution. Data from the Advanced Very High Resolution Radiometer (AVHRR), one of the longest continual series of images of the Earth's surface, have been used to estimate leaf area index (Hunt *et al.*, 1996; Nemani and Running, 1995; 1996), net primary productivity (Goward and Dye, 1987) and land-cover and land-use change (DeFries *et al.*, 1998; 1999; Goward *et al.*, 1985; Loveland *et al.*, 2000; Ramankutty and Foley, 1999a; 1999b; Tucker *et al.*, 1985). These

derived variables are fundamental to modelling the biogeochemical and biogeophysical interactions between the atmosphere and vegetation at intraannual to decadal timescales (Field *et al.*, 1995; Hunt *et al.*, 1996). The shortness of the AVHRR record (the first AVHRR-bearing satellite was launched in 1978), however, thwarts study of longer-term phenomena such as vegetational responses to deglaciation, climatic change, and CO₂ variations at millennial timescales, or changes in land cover resulting from anthropogenic land use within the last several thousand years.

Although the term 'remote sensing' is usually applied to the spaceborne or airborne human-made instruments that intercept electromagnetic radiation reflected or emitted from the earth's surface and transmitted through the atmosphere (Figure 1), remote sensing more generally refers to any set of observations collected by sensors not in direct contact with or close proximity to the observed object (Avery and Berlin, 1992). The pollen rain that is captured and preserved in lake and mire sediments thus is also a

*Author for correspondence (e-mail: williams@nceas.ucsb.edu)

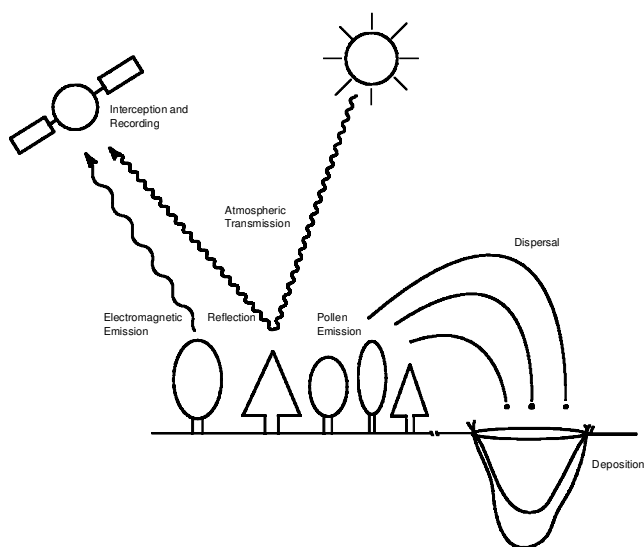


Figure 1 Cartoon illustrating the analogy between a satellite-mounted instrument and a lake (or mire) as remote sensors of the vegetation. The former records the electromagnetic radiation emitted or reflected from the vegetated surface, parsed out into distinct bands or channels, whereas the latter captures pollen emitted from the surrounding vegetation community and dispersed by chance to the lake. For both sensors, the information recorded is an indirect proxy for the properties of interest (e.g., community composition, canopy structure) and the signal received has been distorted during transmission. A challenge common to remote sensing and palaeoecology is to devise algorithms for extracting ecologically meaningful information from remotely sensed observations.

remote sensor of present and past vegetation composition (Prentice, 1988; Webb, 1981; 1993). Fossil pollen records in unglaciated regions can span hundreds of thousands of years (Allen *et al.*, 1999; Tzedakis, 1993) or rarely, millions of years (Hooghiemstra, 1984), enabling studies of vegetation dynamics at timescales not accessible to remote sensing. Syntheses of fossil pollen data have demonstrated the independent responses of plant taxa to past climatic changes (Davis, 1976; Jacobson *et al.*, 1987; Jackson and Overpeck, 2000), and show large variations in the past distribution of plant taxa, biomes and palaeoclimates at millennial timescales (Bartlein *et al.*, 1986; Gajewski *et al.*, 2000; Guiot *et al.*, 1993; Overpeck *et al.*, 1992; Prentice *et al.*, 1991; 1998; 2000; Webb *et al.*, 1993; 1998; Williams *et al.*, 2000).

Satellite-derived and pollen records provide complementary information about vegetation change across a wide range of temporal and spatial scales (Table 1); linking the fossil pollen and satellite-based sensors potentially offers a powerful approach to studying land-cover change at regional to global scales across timescales ranging from years to millennia. The temporal length of fossil pollen records affords the opportunity to study vegetation change at timescales inaccessible to satellite-based sensors. Conversely, remotely sensed observations provide spatially precise information about vegetation structure and land-cover type essential to global change studies. As one example, DeFries *et al.*

(1999) used AVHRR data to map the percent surface area covered by needleleaved woody plants, broadleaved woody plants, and herbs and bare ground at a global scale. By empirically calibrating the modern pollen data against the AVHRR-derived estimates of tree-canopy cover, it should be possible to use the fossil record to extrapolate satellite-derived variables beyond the several decades of direct observation, providing quantitative maps of land-cover change at timescales beyond the several decades of satellite observations. More accurate reconstructions of past land cover can (1) provide a baseline from which to measure effects of postindustrial anthropogenic land use and land-cover change (Ramankutty and Foley, 1998; 1999a) and (2) improve our understanding of atmosphere-vegetation feedbacks at millennial to glacial-interglacial timescales (Prentice and Webb, 1998).

Potential challenges to matching the pollen and AVHRR sensors derive from the fact that each records fundamentally different kinds of information (the AVHRR records five frequency bands of electromagnetic radiation, pollen samples consist of grain counts for 10^1 – 10^2 pollen types) and are differentially sensitive to different aspects of the vegetation (Table 1). Taxa perceived as similar by the AVHRR sensor (e.g., boreal needleleaved trees) may produce very different palynological signals (e.g., *Pinus* tends to be overrepresented in pollen records and *Abies* underrepresented). The spatial resolution of the AVHRR is approximately 1 km, but the spatial resolution of pollen records varies with the size of the collecting basin and dispersability of the various pollen types, with source-area radius ranging between 100 m and 100 km (Bradshaw and Webb, 1985; Calcote, 1995; Jackson, 1990; 1991; Jackson and Kearsley, 1998; Prentice, 1985; 1988; Prentice *et al.*, 1987; Sugita, 1994). The AVHRR has an effective temporal resolution of 10–30 days (Eidenshink, 1992; Eidenshink and Faundeen, 1994), whereas fossil pollen records have a temporal resolution ranging from 10^1 to 10^2 years per sample, depending on rates of sediment accumulation (Webb and Webb, 1988).

In this study we conducted a series of analytical comparisons between AVHRR-derived estimates of percent tree cover (DeFries *et al.*, 1999) and pollen percentages from surface sediment samples in eastern North America, with the goals of empirically quantifying the relationship between the palynological and AVHRR observations of the vegetation, identifying key sources of uncertainty, and developing appropriate techniques for minimizing these uncertainties. For our study area, we chose two regions in eastern North America with strong gradients in vegetation physiognomy and a high density of surface pollen samples. We first aggregated the modern pollen data into needleleaved tree, broadleaved tree and herbaceous categories compatible with the AVHRR tree-cover maps (DeFries *et al.*, 1999) as a heuristic tool for determining which spatial scales and distance weightings provide the best fit between the pollen data and AVHRR estimates of tree cover. Our results are consistent with previous research into pollen source area and transport processes, suggesting that scaling-up to plant life forms does not obscure fundamental pollen-vegetation relationships. The amount of variance in the aggregated pollen data explained by the tree-cover percentages is low, however, due to the higher sensitivity of the palynological sensor to vegetation patterns at <1 km scale and intertaxonomic differences in pollen dispersal and productivity. We show that spatially smoothing the data and using analogue-based approaches can minimize errors arising from these sources of uncertainty. This work sets the stage for future efforts to use palaeoecological data sets to extrapolate satellite-sensed indices of the vegetation (e.g., land-cover type, percent tree cover, LAI) to time periods preceding instrumental remote sensing.

Table 1 Properties of the AVHRR and pollen sensors

	AVHRR	Pollen
Active/passive	Passive	Passive
Spatial resolution	1 km	10 m–100 km
Extent	Global	Global
Temporal resolution	1–30 days	10^1 – 10^2 years
Extent	1982–present	10^2 – 10^6 years
Data resolution	5 spectral channels	10^1 – 10^2 pollen types

Data and methods

Study area

We selected two regions in eastern North America for study, based upon three criteria: (1) well-defined physiognomic gradients from broadleaf-dominated to needleleaf-dominated forests; (2) numerous modern pollen samples; and (3) minimizing the size of the area affected by human land use. The lessons learned with these limited study areas provide a foundation for future analyses of other vegetation types at broader spatial scales.

The first region is set in the northeastern United States and southern Canada (NEUSSC), defined as the area between 41°N and 51°N, and 80°W and 71°W (Figure 2, top). The vegetation ranges from evergreen needleleaf-dominated forests in the north to mixed forests in southern Canada and the northern US, to deciduous hardwood forests covering most of New York and southern New England (Figure 2). Finer-scale transitions in species abundances and plant associations occur within this broad physiognomic gradient (Braun, 1950; Rowe, 1972). In southern New England, the broadleaved deciduous forests are dominated by oak (*Quercus*), hickory (*Carya*), maple (*Acer*) and other hardwood taxa. Pines (*Pinus*) are abundant in sandy coastal and outwash regions (Braun, 1950). The mixed forests in New York and northern New England contain hemlock (*Tsuga*) and white pine (*Pinus strobus*) associated with beech, (*Fagus*), maple, birch (*Betula*) and basswood (*Tilia*), and other minor hardwoods (Braun, 1950). In southern Ontario and Quebec and at high elevations in the Adirondacks (NY) and White Mountains (NH), mixed forests give way to needleleaved forests dominated by spruce (*Picea*), fir (*Abies*), pine and larch (*Larix*). Broadleaved trees are represented by birch, alder (*Alnus*) and poplar (*Populus*) (Rowe, 1972). In the north, total woody cover decreases with latitude as the closed-canopy boreal forest gives way to lichen woodlands (Payette, 1992). Areas deforested by human land use are concentrated around Lakes Ontario and Erie, the eastern seaboard, and along the Hudson and Connecticut River valleys, and are apparent in Figure 2 as low densities of both needleleaved and broadleaved trees.

The second region was set in the southeastern United States (SEUS), delimited to the north and south by the 39°N parallel and the southern US coastline, and to the east and west by 90°W and 78°W (Figure 2, bottom). The gradient from needleleaved-dominated forests to broadleaved-dominated forests runs from south to north, opposite of the NEUSSC trend. Major vegetation types in the SEUS include the mixed and western mesophytic forests, the oak-hickory forest, the oak-pine forest and the southeastern evergreen forest (Braun, 1950; Delcourt and Delcourt, 2000). The mesophytic broadleaved deciduous forests of Kentucky and Tennessee primarily consist of beech, tulip tree (*Liriodendron*), basswood, maple and oak. The southern evergreen forest is dominated by pine (*Pinus palustris*, *P. taeda*, *P. echinata*, *P. elliotii*), accompanied by broadleaved genera such as oak, hickory, magnolia (*Magnolia*), tupelo (*Nyssa*), sweetgum (*Liquidambar*), ash and maple (Braun, 1950; Christensen, 2000). Intermediate between the northern deciduous forest and the southeastern evergreen forest is a broad band of oak-pine forest that covers the Piedmont region of northern Alabama, Georgia, South Carolina and central North Carolina (Braun, 1950; Delcourt and Delcourt, 2000). Low tree-cover densities in Piedmont and central Florida (Figure 2) are due primarily to logging and agricultural use (Christensen, 2000).

Modern pollen data

The surface pollen data in the NEUSSC consisted of 392 surface pollen samples, 318 drawn from the Brown University Surface Pollen Dataset (Avizinin and Webb, unpublished data; Williams, 2000) and 74 additional surface samples from New York

(Jackson, 1990; 1991; unpublished data). Only surface samples from lakes and mires were used. A total of 128 surface pollen samples from the Brown Surface Pollen Dataset were used for the SEUS, of which 69 were from lakes and mires, and 59 were from moss samples. We included the moss samples to improve the pollen site coverage in the SEUS, while recognizing that moss under forest canopies may receive pollen from a smaller source area than lakes and mires (Jackson and Kearsley, 1998; Prentice, 1985). Polsters, however, appear to record not only the local vegetation; previous studies suggest that over 50% of the pollen captured by polsters derived from sources at least 120 m distant (Jackson and Kearsley, 1998; Jackson and Wong, 1994).

A list of 65 pollen types comprising the major woody and herbaceous plant taxa was extracted from the surface samples (Table 2); the same list of taxa was used for the pollen sum. The pollen taxa were classified into life-form categories consistent with the tree-cover density maps (DeFries *et al.*, 1999): broadleaved trees and shrubs, needleleaved trees and shrubs and non-arboreal taxa (Table 2).

Land-cover type for each pollen sample location was determined from the DISCover data set, International Geosphere-Biosphere Programme (IGBP) classification (Loveland *et al.*, 2000). A search window measuring 20 × 20 km was placed around each location and the modal land-cover type retained. Of the 17 IGBP land-cover types, three represent vegetation modified by human use: 'Croplands', 'Urban and Built-Up' and 'Cropland/Natural Vegetation Mosaic'. Pollen sites assigned to these three categories were included for display in Figure 2, but were discarded before subsequent analyses.

Modern tree cover

The AVHRR-derived estimates of percent broadleaved and needleleaved tree-canopy cover used here were produced by DeFries *et al.* (1999), who provide a full description of the methods used. A linear mixture model was applied to an AVHRR data set spanning 1 April 1992 to 31 March 1993 (Eidenshink and Faundeen, 1994) in order to estimate, for each pixel, the percent area covered by woody vegetation, herbs and bare ground. The woody vegetation was further classified into (1) needleleaved versus broadleaved trees and (2) evergreen versus deciduous trees. For North America, the two subclassifications were assumed to be equivalent, with the woody vegetation classified into needleleaved evergreen and broadleaved deciduous trees. Deciduous needleleaved and broadleaved evergreen woody taxa are relatively minor constituents of the North American vegetation although they may be regionally important, e.g., in the subtropical flora of Florida or the California chaparral. The classification of woody shrubs varied with their height: low-lying shrubs tended to be classified as herbaceous cover, and taller shrubs as woody plants. Because the mixture model was less accurate at upper and lower extremes of woody plant abundances, minimum and maximum values for the percent pixel area occupied by woody vegetation were defined: estimated coverages less than 10% were set to 0%, and coverages greater than 80% were set to 80% (DeFries *et al.*, 1999).

Analyses and results

Overview

We present our results as a chain of analyses in which the findings at earlier stages motivate subsequent work. We begin by comparing the aggregated pollen percentages for needleleaved and broadleaved taxa to the AVHRR tree-cover percentages (Figures 2–4). Mapped overlays of the pollen percentages against the AVHRR tree-cover percentages (Figure 2) show that both sensors capture the first-order gradients in physiognomy, as well as second-order features corresponding to regional topographic variations. We

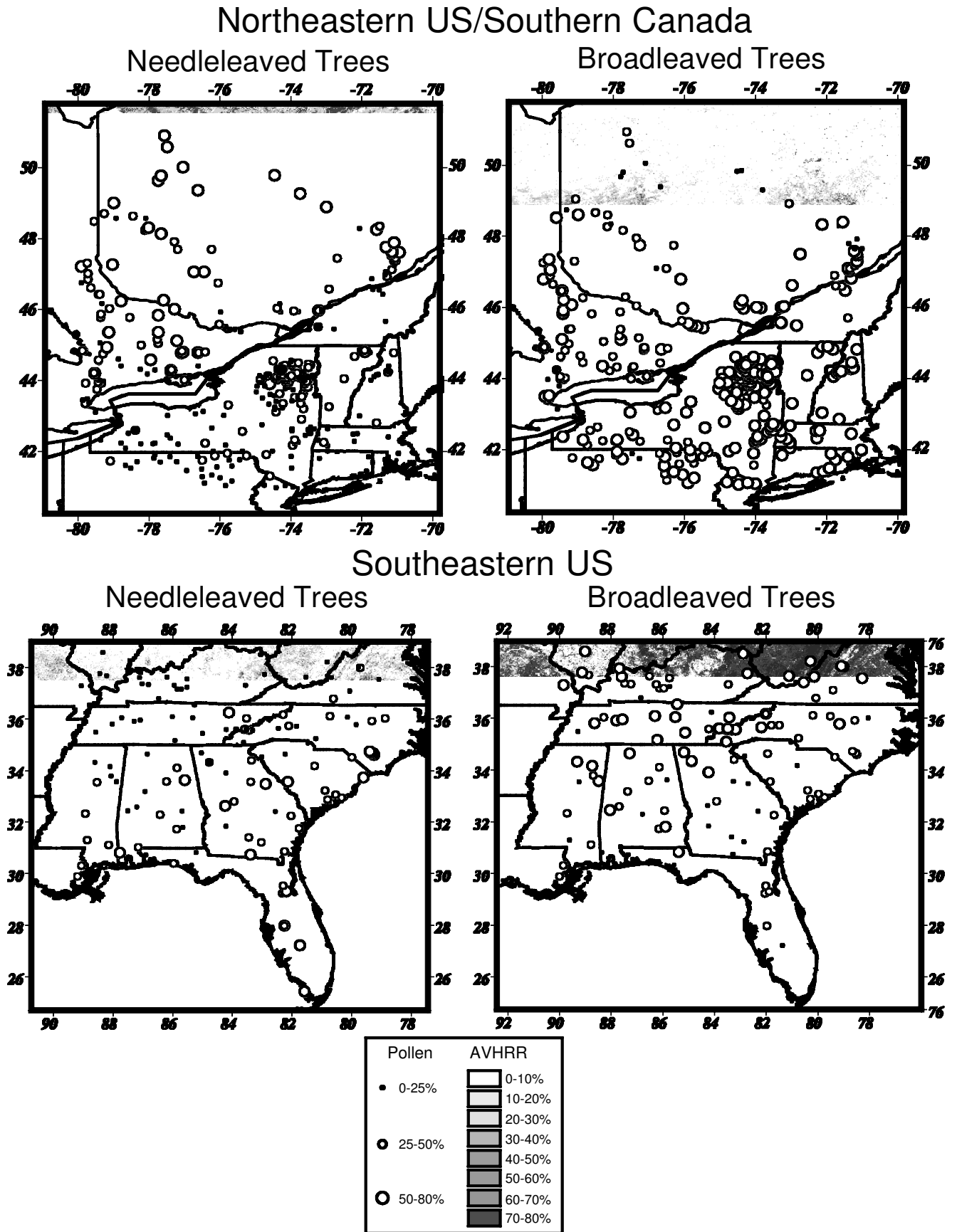


Figure 2 AVHRR-derived estimates of broadleaved and needleleaved tree abundances in the northeastern US and southern Canada (NEUSSC), and the southeastern US (SEUS) (DeFries *et al.*, 1999). Percentages refer to the percent pixel cover of each plant life form. The dots mark the locations of surface pollen samples. Note that each dot has a radius of approximately 20 km.

Table 2 Classification of pollen types into life-form categories (DeFries *et al.*, 1999)

Category	Pollen type
Broadleaved tree/shrub	<i>Acer</i> , <i>Alnus</i> , Aquifoliaceae, <i>Betula</i> , <i>Carya</i> , <i>Castanea</i> , <i>Ceanothus</i> , <i>Celtis</i> , <i>Cephalanthus</i> , <i>Cercocarpus</i> , <i>Clethra</i> , <i>Corylus</i> , <i>Empetrum</i> , Ericaceae, <i>Fagus</i> , <i>Fraxinus</i> , <i>Juglans</i> , <i>Liquidambar</i> , <i>Mimosa</i> , Myricaceae, <i>Nyssa</i> , <i>Ostrya/Carpinus</i> , <i>Platanus</i> , <i>Populus</i> , <i>Quercus</i> , <i>Salix</i> , <i>Shepherdia</i> , <i>Tilia</i> , <i>Ulmus</i>
Needleleaved tree/shrub	<i>Abies</i> , Cupressaceae/Taxaceae, <i>Picea</i> , <i>Pinus</i> , <i>Taxodium</i> , <i>Thuja</i> , <i>Tsuga</i> , <i>Larix/Pseudotsuga</i>
Non-arboreal	<i>Ambrosia</i> , Apiaceae, <i>Artemisia</i> , Asteraceae (Tubuliflorae), Brassicaceae, Caryophyllaceae, Chenopodiaceae/Amaranthaceae, Cyperaceae, <i>Dryas</i> , <i>Ephedra</i> , <i>Eriogonum</i> , Euphorbiaceae, <i>Oxyria</i> , Poaceae, Ranunculaceae, Rubiaceae, <i>Sarcobatus</i> , Saxifragaceae, <i>Sphaeralcea</i>

investigate the appropriate spatial scale and distance measure for comparing the pollen and tree-cover data (Figures 3 and 4). Linear regressions against the tree-cover percentages explain less than half of the variance in the aggregated pollen data, motivating subsequent analyses designed to identify and minimize key sources of uncertainty. Two primary sources are identified: the sensitivity of pollen records to local variability in the vegetation and inter-taxonomic differences in pollen representation. Subsequent analyses (Figures 5–7) show that each can be minimized by appropriate choice of method. Specifically, we minimize the effects of local variability by smoothing the pollen data (Figure 5) and the effects of differential pollen production and representation (Figure 6) by using modern-analogue methods (Figure 7).

Spatial distribution of needleleaved and broadleaved pollen and trees

In the NEUSSC, the gradient from high percentages of coniferous pollen types in northern surface samples to high percentages of broadleaved types in southern surface samples mirrors the physiognomic gradient from the conifer-rich Canadian boreal forest to the broadleaved deciduous forests of New York and New England (Figure 2, top). The relatively sparse set of pollen sites cannot match the detailed resolution of the AVHRR data, but is able to resolve regional features such as the high abundances of needleleaved trees in the Adirondacks. The pollen and AVHRR maps are most discrepant in eastern Ontario, where several sites have high percentages of pollen from broadleaved trees but the AVHRR reconstructions indicate high percentages of needleleaved tree cover. The discrepancy is largely caused by high abundances of birch pollen (Webb *et al.*, 1983), which is heavily over-represented in mixed northern forests (Bradshaw and Webb, 1985; Jackson, 1990; Prentice *et al.*, 1987).

In the SEUS, the gradient from high percentages of broadleaved pollen in the north (chiefly oak and hickory) to high abundances of needleleaved pollen types in the south (pine) is consistent with the observed trend from broadleaved deciduous forests in Kentucky and Tennessee to coniferous southern mixed forest (Figure 2). Second-order features such as the elevated abundances of needleleaved trees in the Appalachian Mountains (Figure 2, bottom) and along the coast are discernible from the pollen data. Again, the main limitation for resolving finer-scale features is the low site density relative to the AVHRR observations. The pollen and AVHRR data are most discrepant in southern Florida, where the pollen samples include high abundances of coniferous pollen types and the AVHRR indicates low percent coverages for both

broadleaved and needleleaved trees. The pollen bias towards high needleleaved abundances in Florida may be due to an over-representation of pine in the pollen samples, or may be due to human alteration of the Florida vegetation, which consists of a mosaic of cropland and natural vegetation (Loveland *et al.*, 2000). Most Florida surface samples were not used in the following analyses, because of the heavy anthropogenic modification of the vegetation (see methods above).

Evaluating the spatial scale of the relationship between the AVHRR and pollen data

To compare the AVHRR estimates of tree cover and aggregated pollen percentages across a range of spatial scales, a square search window of variable size (search window half-widths of 1, 5, 10, 25, 50, 75, 100, 150, 200 and 250 km) was centred on each pollen site and the AVHRR-estimated evergreen and broadleaved tree-cover percentages from all pixels within the window were averaged. Search windows were permitted to extend beyond study-area boundaries. AVHRR pixels over water bodies 1 km² in size or greater were removed by application of a water mask derived from the DISCover land-cover map. We experimented with unweighted, inverse-distance (1/D) and inverse-distance-squared (1/D²) weightings of the AVHRR pixels. For each set of plots, we fitted linear regressions and report the percent variance explained (r^2). Use of linear regression facilitates comparisons among plots, but we recognize that using percentage data for a limited number of types may introduce non-linearities (Prentice and Webb, 1986) not accommodated by simple linear models.

A positive monotonic relationship exists between the percent pollen abundances for the needleleaved and broadleaved trees and their AVHRR-estimated coverages (Figure 3). As the search window size increases, the slope of the best-fit linear regression increases and the y-intercept decreases (Figure 3), consistent with previous findings that the y-intercept should decline as an increasing proportion of the pollen source area is encompassed by the search window (Bradshaw and Webb, 1985; Prentice *et al.*, 1987). However, the NEUSSC and SEUS each include several vegetation zones with different species associations, so the proportion of background pollen across sites is unlikely to be uniform. The amount of variance in the aggregated pollen percentages explained by the AVHRR tree-cover percentages is relatively poor at small spatial scales (window half-width <25 km) but increases rapidly and levels off between 25 and 75 km (Figure 4). Maximal r^2 values are moderate to low, ranging between 0.3 and 0.4.

The general shape of the r^2 curve (increasing rapidly at small spatial scales and levelling off between 25 and 75 km) is robust to the choice of distance weightings (Figure 4). The unweighted and inverse-distance weightings result in regressions that explain more variance than the inverse-distance-squared weighting at short to intermediate spatial scales (<50–75 km) but less variance is explained at larger spatial scales. The r^2 curves for the 1/D² weighting consistently increase rapidly then level off, whereas the curves for the unweighted and 1/D weightings tend to peak between 25 and 75 km, and can either increase or decrease slowly at larger spatial scales. These patterns are consistent across regions and life forms.

Although a positive relationship exists between the percent pollen abundances of needleleaved and broadleaved tree taxa and the AVHRR tree-cover estimates, the majority of the variance in the pollen data is not explained by the tree-cover percentages (Figure 4). Simply aggregating pollen data into life-form categories alone does not provide an adequate proxy for tree cover.

Filtering local-scale variability from the pollen data

Smoothing the pollen data set removes site-specific variability in the pollen data (Graumlich and Davis, 1993) resulting from stand-scale sources of pollen not resolvable in the AVHRR data. We

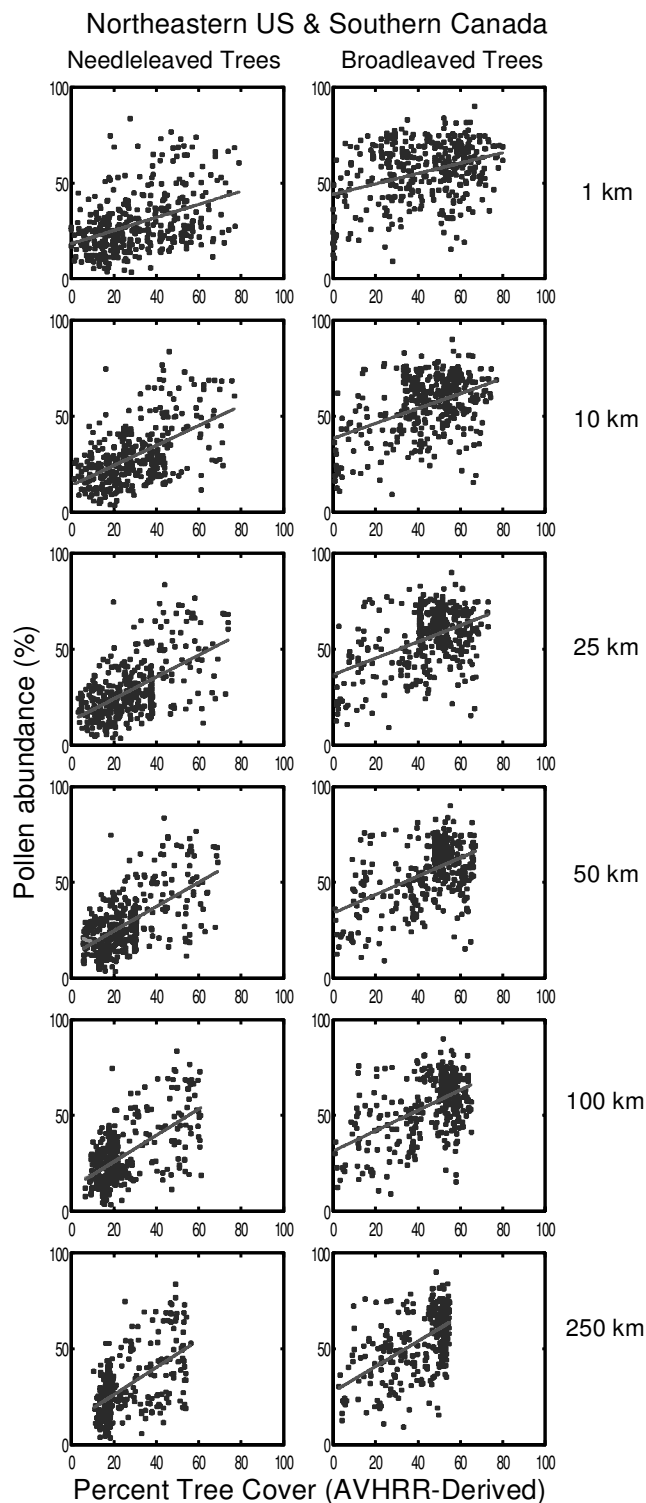


Figure 3 Scatterplots comparing the percent abundance of needleleaved pollen types to AVHRR-derived tree-cover percentages for the NEUSSC. The AVHRR values were obtained by placing a search window around each pollen site that ranged in half-width from 1 km to 250 km and averaging the unweighted values for all pixels within the window. Because the differences between the NEUSSC and SEUS are small relative to the differences between the needleleaved and broadleaved trees, only the NEUSSC plots are shown. The dense cluster of points in the lower left of the needleleaved tree plots and the upper right of the broadleaved tree plots is located in the densely sampled Adirondack Mountains (Figure 2).

spatially smoothed the pollen data set to a $1^\circ \times 1^\circ$ grid resolution, centring a $3^\circ \times 3^\circ$ search window on each gridpoint and weighted-averaging the pollen percentages from all sites within the window using the tri-cube weight function (Webb *et al.*,

1993). The actual grid cell dimensions vary by latitude, but all lie within the optimal spatial scales identified in the prior analysis. The AVHRR estimates of abundance were averaged (unweighted) for all pixels in the gridcell. The smoothing reduces noise due to local variations in pollen signal and ensures a common spatial resolution for the pollen and AVHRR data.

The gridded pollen data (Figure 5) show an improved fit to AVHRR tree coverages ($r^2 = 0.51\text{--}0.60$) compared to the ungridded pollen data (Figure 4). The gridded pollen percentages are also consistent with the DISCover IGBP land-cover classification (Loveland *et al.*, 2000). For example, needleleaf pollen percentages are low in gridcells assigned to the Broadleaf Deciduous Forest, intermediate in the Mixed Forest and high in the Needleleaf Evergreen Forest. Thus, the modern pollen percentages, after smoothing, are in good agreement with vegetation maps produced by two different treatments of the AVHRR data (DeFries *et al.*, 1999; Loveland *et al.*, 2000).

Intertaxonomic differences in sensor sensitivity

A second source of error resides in differences in the sensitivity of the pollen and AVHRR sensors at the level of individual plant taxa. Some taxa tend to be overrepresented in surface pollen samples relative to their abundance in the surrounding vegetation due to high pollen productivities, amenability to wind dispersal and/or resistance to degradation; other taxa are underrepresented (Bradshaw and Webb, 1985; Prentice *et al.*, 1987; Webb and McAndrews, 1976). The AVHRR sensor may also be differentially sensitive to plant species based upon their position in the canopy, with canopy species likely to be better represented than those found in the understorey. The interplay between the differential sensitivities of the two sensors weakens the correlation between the aggregated pollen percentages and AVHRR estimates of percent tree cover.

The importance of this effect is shown in Figure 6, which replots the data from Figure 3 as graduated circles whose diameters are scaled to the percent abundance of a pollen type relative to all taxa belonging to its plant life form. This figure shows (a) whether the distribution of an individual pollen type is characteristic of its life-form category and (b) whether differences in sensor sensitivity for this taxon are a likely source of variance. The distribution of the graduated circles falls into five general cases. First, the size of the graduated circles may be uniform or display no coherent pattern (e.g., pine, oak and hickory in the SEUS), indicating that the percent pollen abundance of a plant taxon occupies a generally constant fraction of the aggregate pollen abundance of its life form, and is thus a good indicator of the overall abundance of its life form. Second, the largest values may occur in the upper-right quadrant, suggesting that the plant taxon typically associates with other taxa of similar life form (e.g., oak and beech in the NEUSSC are most abundant in broadleaved deciduous and mixed mesophytic forests; spruce is most abundant in the boreal forest). Third, the largest values may occur in the lower-left quadrant, suggesting that the plant taxon typically associates with other taxa of different life form (e.g., hemlock and Cupressaceae). The second and third cases suggest that the pollen and AVHRR sensors are similarly sensitive to the taxon. Fourth, the largest values may occur in the upper-left quadrant, indicating that the plant taxon is overrepresented in the pollen data relative to the AVHRR tree-cover maps (e.g., birch and alder in the NEUSSC and sweetgum in the SEUS). Fifth, the largest values may occur in the lower-right quadrant, indicating that the plant taxon is underrepresented in the pollen data relative to the AVHRR tree-cover maps (e.g., fir and maple, and spruce at some sites). The fourth and fifth cases suggest differences in the sensitivity of the pollen and AVHRR sensors that degrades the general fit between the observations.

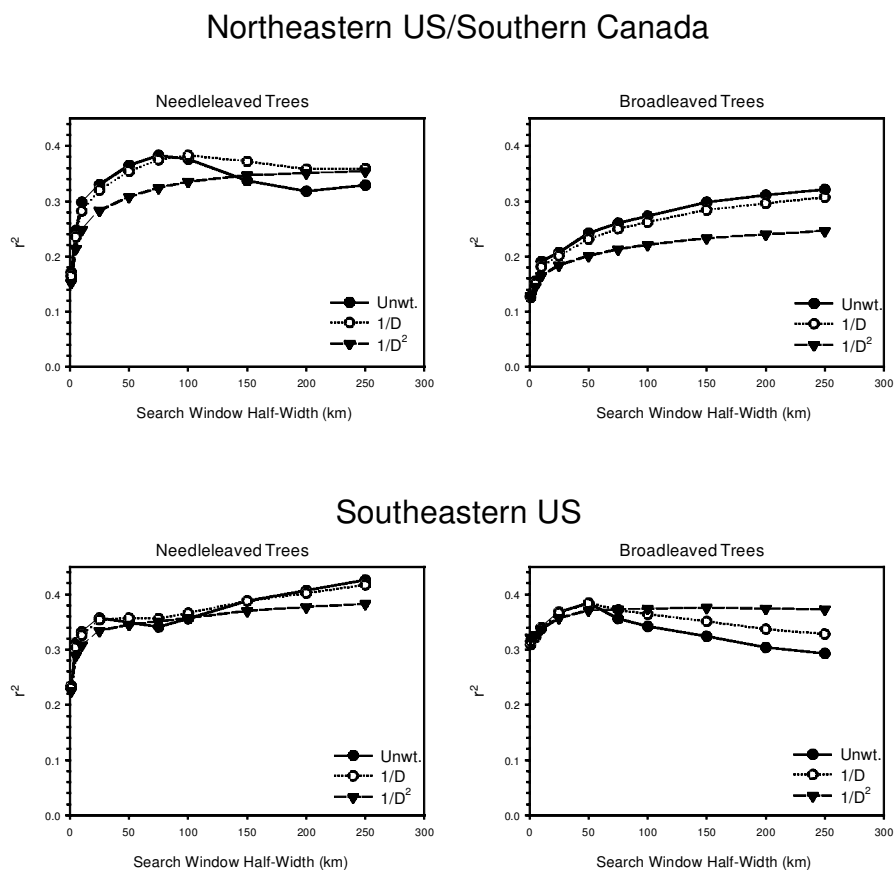


Figure 4 The proportion of variation in the percent pollen abundances of needleleaved and broadleaved taxa in surface pollen samples explained by AVHRR-derived tree-cover estimates in the NEUSSC and SEUS across a range of spatial scales and with three different distance weightings: unweighted, $1/D$ and $1/D^2$. The unweighted curve (solid line with circles) summarizes the data shown in Figure 3.

Modern analogue technique

Modern analogue approaches offer a way to circumvent inter-taxonomic differences in sensor sensitivity. Rather than seeking to correlate the aggregate life-form pollen percentages to the AVHRR estimates of tree cover, an analogue-based approach estimates the percent tree cover for a pollen sample based on the tree-cover percentages at sites with similar pollen spectra. This approach reduces the information loss inherent in aggregating the pollen taxa into a few life-form categories by using the full pollen spectra to assess similarity between sites. Application of the modern analogue technique in this context assumes that similarly composed pollen samples were produced by floristically and physiognomically similar plant associations (Overpeck *et al.*, 1985; 1992). The accuracy of the approach can be evaluated for the modern data by comparing the observed AVHRR tree-cover values at each surface sample location to the tree-cover percentages associated with the most similar surface samples.

We used a standard variant of the modern analogue technique in which each pollen sample was compared to all other modern pollen samples, using the squared-chord distance (SCD) to quantify similarity (Overpeck *et al.*, 1985; Prentice, 1980). SCDs had to be less than 0.15 for a sample to be identified as a viable analogue (Overpeck *et al.*, 1985). A maximum of 10 analogues was permitted for each surface pollen sample, from which average needleleaf and broadleaf cover percentages were calculated. If a surface pollen sample had no viable analogue, it was discarded from the analysis. We allowed the set of potential modern analogues to span a wider range of environments than that encompassed by the study area, using a North American pollen data set comprising 3335 pollen samples (Avizinis and Webb, 1985; Williams, 2000). A pollen sample was not permitted to match to itself.

We found a close agreement between the observed tree-cover percentages and the best-analogue reconstructions (Figure 7). The observed tree-cover percentages explain 70% of the variance in the best-analogue needleleaved tree-cover percentages and 78% of the variance in the best-analogue broadleaved tree-cover percentages. The standard error of the analogue estimates is 7.0% for needleleaved trees and 7.7% for broadleaved trees.

Discussion

The central challenge for palynologists is to interpret the raw counts of fossil pollen grains in ecologically relevant terms. This endeavour is directly analogous to the efforts in the remote-sensing community to develop algorithms to infer land-surface properties from the numbers and frequencies of photons captured by airborne and spaceborne instruments. Together, satellite-sensed and palynological data provide a powerful tool for exploring vegetational and land-cover change at timescales not accessible by the satellite record alone and for vegetation properties not easily inferred by other means. Here, we have studied the relationship between tree-cover percentages as inferred from phenological analyses of AVHRR observations with the distribution of needleleaved and broadleaved pollen types in modern sediments. Our findings suggest that the modern distributions of needleleaved and broadleaved pollen types are broadly consistent with the corresponding tree-cover percentages, and that the fit is markedly improved by spatially smoothing the pollen data and using analogue-based approaches to reconstruct the modern vegetation. This initial exploration of data and methods paves the way for future palaeoecological applications. Our methods and analyses can easily be extended to other regions, with the main limitation

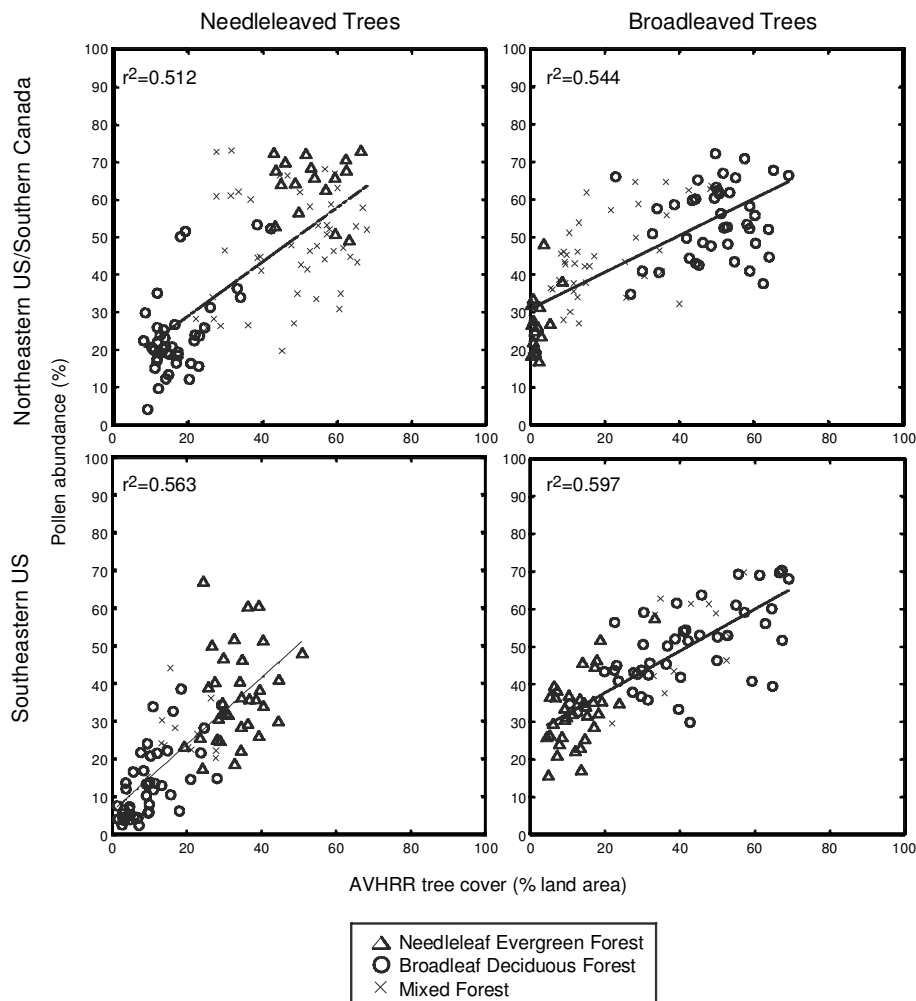


Figure 5 Scatterplots comparing the AVHRR tree-cover percentages and pollen percentages after smoothing and interpolating both data sets to a $1^\circ \times 1^\circ$ grid. The proportion of variance explained for the gridded observations is significantly improved over those for individual pollen sites (Figure 4), suggesting that local-site variability in the pollen data can be minimized with the appropriate filter. Individual gridpoints are labelled according to their DISCover biome type, using the IGBP classification system (Loveland *et al.*, 2000).

being the availability of surface pollen data. Dense modern data sets exist for North America, Europe (Guiot *et al.*, 1993; Peyron *et al.*, 1998), western Russia (Tarasov *et al.*, 1998), and China (Yu *et al.*, 2000), and collection efforts continue for other parts of the globe. In the following discussion, we review potential sources of error in the pollen-AVHRR regressions and the appropriate analytical techniques for minimizing error, and discuss future prospects for linking palaeoecological and instrumental remote sensors.

Reconciling the palynological and AVHRR sensors: assessing and reducing errors and uncertainties

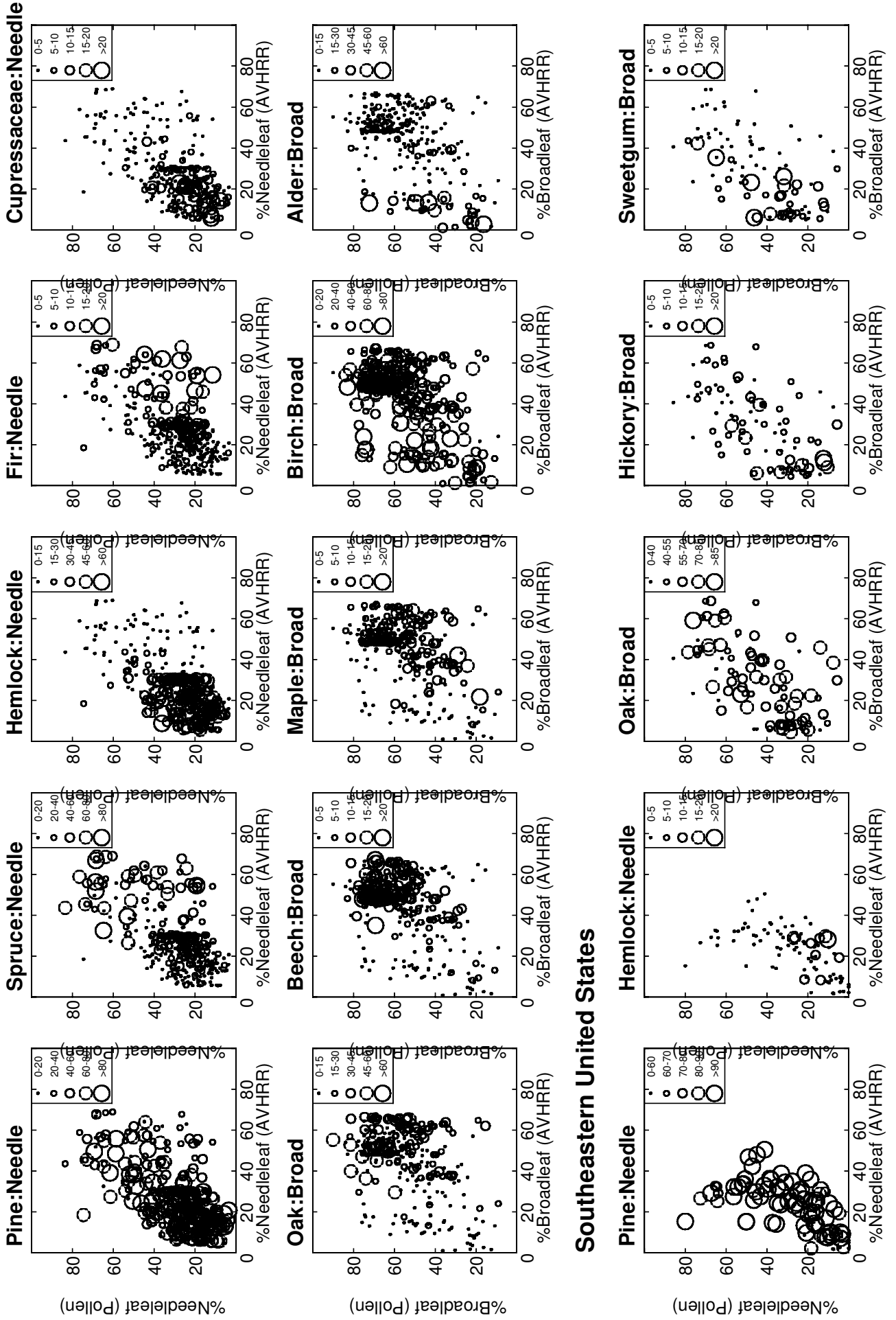
We are trying to reconcile two contrasting sensor systems, each of which records different aspects of the vegetation at overlapping but not identical temporal and spatial scales (Table 1). In this section we assess the sources of error, uncertainty and mismatch between the two sensing systems; identify which are trivial and which are important; and determine which can be mitigated by choice of analysis. Potential sources of error in the pollen-AVHRR plots (Figures 3 and 4) include (from lesser to greater importance) uncertainties of spatial location, temporal discrepancies between the pollen and AVHRR data, uncertainties in the AVHRR classification, determining the appropriate pollen source-area and distance-weighting function, and noise arising from the grouping of disparate taxa into broad morphological categories. In particular, summing pollen percentages into plant life forms is challenged by the differential representation of plant taxa in pollen

records, caused by intertaxonomic differences in pollen productivity and dispersability. We have shown, however, that with appropriate analytical approaches the major sources of uncertainty can be minimized or eliminated.

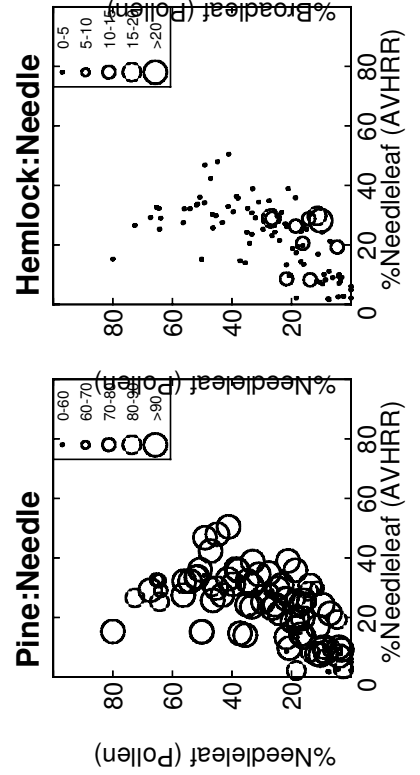
The precision of the spatial coordinates of the surface pollen samples is a relatively minor source of uncertainty. Pollen sample locations typically are stored in databases as latitude/longitude coordinates, with a precision of 0.01 degrees. This is equivalent, in the mid-latitudes, to an approximate precision of approximately ± 1 km. The accuracy of the AVHRR geometric registration is slightly greater than 1 km (Eidenshink and Faundeen, 1994), so that a pollen site cannot be confidently matched to a specific AVHRR pixel. This uncertainty, however, is minor given a 25–75 km pollen source radius (Figure 4).

Figure 6 The data plotted in this figure are identical to those in Figure 3, using a 50 km half-width search window and no distance weighting. The diameter of the graduated circles corresponds to the ratio of the percent abundance of a given pollen type against all pollen types assigned to its life form. Comparison of the distribution of the large circles (i.e., sites where the pollen type constitutes a large fraction of the total pollen sum for its life form) against the distribution of all sites provides information about (1) whether the pollen type is associated with high abundances of its life form and (2) whether the pollen type tends to be over- or under-represented in modern pollen samples relative to AVHRR estimates of percent tree cover.

Northeastern United States & Southern Canada



Southeastern United States



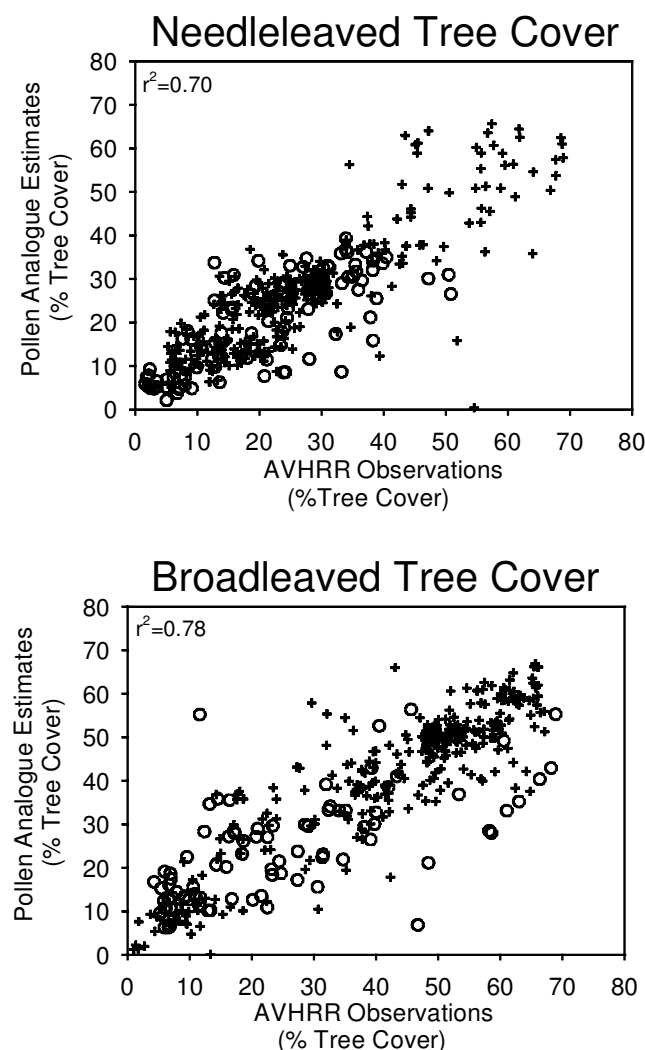


Figure 7 Scatterplots of the observed values of needleleaved and broadleaved tree-cover percentages (AVHRR) versus the average tree-cover percentages at sites with similar modern pollen spectra. Crosses indicate NEUSSC surface samples; circles indicate SEUS surface pollen samples.

The palynological and AVHRR observations were collected at different times, and hence may represent slightly different states of the vegetation. Most of the surface pollen data used in this study were published in the 1960s and 1970s, with the earliest published in the 1940s and the most recent in the early 1990s (Avizinin and Webb, unpublished data). Thus, an average discrepancy of approximately two decades exists between the palynological and AVHRR observations. This discrepancy is short relative to the temporal resolution of most pollen records (Webb, 1993) and the time constant of most natural processes governing the composition and structure of eastern forests. However, regions recently altered by natural or anthropogenic disturbances or reforestation following cropland/pasture abandonment may degrade the match between the AVHRR and palynological observations. The size of this uncertainty is difficult to measure, but we have minimized it by eliminating surface pollen samples from regions most affected by human land use (Loveland *et al.*, 2000).

A second source of temporal uncertainty arises from the differing resolutions of the two sensors. The temporal resolution of pollen samples collected from the top of a lake sediment column ranges from 0.5 to 100 years per sample, with a mean of 7 years/cm³ (Webb and Webb, 1988). Thus, the sedimentary processes underlying the palynological record tend to smooth out interannual variations, so that each sample represents a decadal-scale integration of the vegetation (Webb, 1993). The tree-cover

maps used here are based on 16 months of AVHRR observations (DeFries *et al.*, 1999). Interannual variability in AVHRR observations between 1982 and 1994 resulted in a 5–10% standard deviation in the estimates of percent woody cover (DeFries *et al.*, 2000), attributed to interannual variations in the transparency of the atmosphere.

The uncertainty of the AVHRR observations against the actual percent vegetation cover is not yet well known: ground-truthing of the woody vegetation percentages has been limited due to the lack of extensive land-surface observations at the appropriate scale. The estimates are, however, consistent with other remotely sensed land-cover data sets (DeFries *et al.*, 1999).

A standard source of error in interpreting palynological data arises from uncertainties of the pollen source area and distance. Whereas the AVHRR-derived tree-cover data sets have a fixed resolution of 1 km, each pollen site integrates pollen inputs across a source area that varies among sites, due to differences in local geomorphology, and among taxa within a site, due to differences in pollen dispersability (Calcote, 1995; Jackson and Kearsley, 1998; Prentice, 1988; Sugita, 1994; Sugita *et al.*, 1999; Jackson and Lyford, 1999). Based on the observed peak in variance explained (Figure 4), we estimate an average pollen source radius of 25–75 km. This estimate is consistent with previous values calculated from studies of individual taxa (Bradshaw and Webb, 1985; Delcourt *et al.*, 1984; Jackson, 1991; Prentice *et al.*, 1987; Webb, 1974, Webb and McAndrews, 1976), indicating that scaling up from individual taxa to plant life forms does not alter the estimated pollen source area. The peak in r^2 at 250 km for the broadleaved trees in the NEUSSC and the needleleaved trees in the SEUS (Figure 4) is a statistical artifact resulting from the tendency of pollen-vegetation regression lines to steepen with increasing spatial scale (Figure 3). Our finding that unweighted or inverse distance weightings produce the best fit between the pollen and AVHRR data at short to intermediate distances (<75 km) suggests that within the pollen source area the regional pollen rain is fairly well homogenized. By placing a strong weighting on nearby locations, the $1/d^2$ weighting is approximately equivalent to using a 1 km radius with minor modification from outer radii (Jackson and Kearsley, 1998).

The most significant source of noise in the AVHRR-pollen comparisons is grouping the pollen taxa into plant life forms, because it masks intertaxonomic differences in pollen representation (Figure 3). In the NEUSSC, sites in the boreal forest tend to have high abundances of broadleaved pollen types relative to the AVHRR-derived estimates of tree cover, primarily due to high abundances of birch and alder pollen (Figures 2 and 6). Birch and alder are highly overrepresented in modern pollen samples from boreal regions (Bradshaw and Webb, 1985; Jackson, 1990; Prentice *et al.*, 1987) due to high pollen productivity and dispersability. Conversely, the AVHRR sensor may be relatively insensitive to birch and alder if they grow in an understorey or shrub habit. Many tree taxa are severely underrepresented in pollen records (e.g., *Liriodendron*, *Magnolia*) and so represent trees that the AVHRR camera ‘sees’ and the surface pollen samples largely do not.

Prospects for using remote sensing data in palaeoecology

Our analysis shows that the larger errors can be eliminated or minimized with appropriate choices of method. A major source of variance in Figure 3 is intertaxonomic differences in pollen productivity and dispersal, resulting in varying degrees of over- and underrepresentation in the modern pollen record. Summing the pollen taxa into plant life forms for comparison against the AVHRR data is a useful heuristic tool, but the observed fit is clearly too poor for palaeoecological application. This problem should worsen at broader spatial scales as interregional differences

in taxonomic composition become more pronounced. Multivariate techniques such as the modern analogue technique (Overpeck *et al.*, 1985), response surfaces (Bartlein *et al.*, 1986; Prentice *et al.*, 1991) or eigenvector-based approaches (Imbrie and Kipp, 1971; Webb, 1974) overcome differences in pollen representation, by comparing pollen samples directly and assuming that similar processes produced similar pollen assemblages. We find a very good agreement between the observed tree-cover percentages and their best-analogue estimates. A challenge for any analogue-based approach is fossil pollen assemblages with no modern analogue (Williams *et al.*, 2001). One solution may be to group pollen taxa according to plant function and/or form, when no good compositional analogues exist for a fossil pollen sample (Williams, 2003).

The agreement between the pollen and AVHRR data is strengthened when both are grouped into $1^\circ \times 1^\circ$ grid cells (Figure 5), indicating that a key component of variation is due to local heterogeneities in the pollen data not resolvable at 1 km scale. The pollen accumulated in lake and mire samples derives from sources spanning a wide range of distances (10^{-2} to 10^3 km). The relative importance of regional versus local sources depends on basin size (Prentice, 1985) but all surface pollen samples include some local vegetational signal that is essentially invisible to the AVHRR. Spatially filtering the pollen data removes this local signal (Graumlich and Davis, 1993; Webb, 1993; Webb and McAndrews, 1976).

Using modern pollen samples and AVHRR-derived tree-cover maps from eastern North America, we have shown that there are no serious obstacles to the use of satellite-derived vegetation data sets in pollen-vegetation studies. The ready availability, low cost and synoptic scope of remotely sensed data sets make them a highly valuable tool for calibration of palaeoecological records. We have presented results from one set of derived data sets; other relevant products include categorical land-cover classifications (DeFries and Townsend, 1994; Loveland *et al.*, 2000), net primary productivity (Goward and Dye, 1987) and leaf-area index (Fassnacht *et al.*, 1997; van Leeuwen *et al.*, 1997). To the extent that these variables are determined by plant-community composition, they also may be amenable to calibration against modern pollen data. AVHRR data are an integral input for a suite of process-based terrestrial biogeochemistry models (Field *et al.*, 1995; Hunt *et al.*, 1996). As the spectral and spatial precision of satellite-based instruments improves, so will the accuracy and resolution of remotely sensed land-cover data sets. Land-cover maps derived from multiyear AVHRR data sets are being developed (DeFries *et al.*, 2000), minimizing the uncertainty caused by interannual variability in the AVHRR observations. The Moderate Resolution Imaging Spectrometer (MODIS), launched in December 1999, improves upon the AVHRR both in spatial and spectral resolution, and should enable more precise vegetation classifications. For regional and landscape-scale studies, high-resolution sensors such as the Landsat Thematic Mapper and Système Pour l'Observation de la Terre already exist and can be used to calibrate palaeoecological records (Allen and Huntley, 1999).

We are currently using the insights gained in this regional study of modern pollen and tree-cover percentages to develop a series of tree-cover reconstructions for North America for the late Quaternary (Williams, 2003). Good-quality maps of past vegetation are needed (Kohfeld and Harrison, 2000; Prentice and Webb, 1998) to provide (1) more realistic inputs to terrestrial biogeochemistry models and general circulation models employing prescribed land-cover maps and (2) validation data sets for coupled vegetation-atmosphere models (e.g. Levis *et al.*, 1999). Continuous-field maps of tree cover have several important advantages over categorical land-cover maps (DeFries *et al.*, 1999): they more accurately represent gradients within the vegetation, they enable a fuller representation of vegetation heterogeneity, and they avoid

semantic differences among classification schemes. By using fossil pollen records to extend satellite-derived measurements of the vegetation to more distant time periods, we hope to understand the impacts of past land-cover changes upon the global carbon cycle and climate.

Acknowledgements

The senior author was supported by a Postdoctoral Fellowship at the National Center for Ecological Analysis and Synthesis, a Center funded by NSF (Grant DEB-94-21535), the University of California – Santa Barbara, the California Resources Agency, and the California Environmental Protection Agency. This manuscript was improved by discussions with A. Elmore, T. Webb, R. DeFries and R. Hunt, and critical comments from T. Webb, E. Grimm and an anonymous reviewer.

References

- Allen, J.R.M. and Huntley, B. 1999: Estimating past floristic diversity in montane regions from macrofossil assemblages. *Journal of Biogeography* 26, 55–73.
- Allen, J.R.M., Brandt, U., Brauer, A., Hubberton, H.-W., Huntley, B., Keller, J., Kraml, M., Mackensen, A., Mingram, J., Negendank, J.F.W., Nowaczyk, N.R., Oberhänsli, H., Watts, W.A., Wulf, S. and Zolitschka, B. 1999: Rapid environmental changes in southern Europe during the last glacial period. *Nature* 400, 740–43.
- Avery, T.E. and Berlin, G.L. 1992: *Fundamentals of remote sensing and airphoto interpretation*. Upper Saddle River, NJ: Prentice Hall, 472 pp.
- Bartlein, P.J., Prentice, I.C. and Webb, T. III 1986: Climatic response surfaces from pollen data for some eastern North American taxa. *Journal of Biogeography* 13, 35–57.
- Bradshaw, R.H.W. and Webb, T. III 1985: Relationships between contemporary pollen and vegetation data from Wisconsin and Michigan, USA. *Ecology* 66, 721–37.
- Braun, E.L. 1950: *Deciduous forests of eastern North America*. New York: Blakiston, 596 pp.
- Calcote, R. 1995: Pollen source area and pollen productivity: evidence from forest hollows. *Journal of Ecology* 83, 591–602.
- Christensen, N.L. 2000: Vegetation of the southeastern coastal plain. In Barbour, M.G. and Billings, W.D., editors, *North American terrestrial vegetation* (second edition), Cambridge: Cambridge University Press, 397–448.
- Davis, M.B. 1976: Pleistocene biogeography of temperate deciduous forests. *Geoscience and Man* XIII, 13–26.
- DeFries, R.S. and Townshend, J.R.G. 1994: NDVI-derived land cover classifications at a global scale. *International Journal of Remote Sensing* 15, 3567–86.
- DeFries, R.S., Hansen, M.C. and Townshend, J.R.G. 2000: Global continuous fields of vegetation characteristics: a linear mixture model applied to multi-year 8 km AVHRR data. *International Journal of Remote Sensing* 21, 1389–414.
- DeFries, R., Hansen, M., Townshend, J.R.G. and Sohlberg, R. 1998: Global land cover classifications at 8 km spatial resolution: the use of training data derived from Landsat imagery in decision tree classifiers. *International Journal of Remote Sensing* 19, 3141–68.
- DeFries, R.S., Townshend, J.R.G. and Hansen, M.C. 1999: Continuous fields of vegetation characteristics at the global scale at 1-km resolution. *Journal of Geophysical Research* 104, 16911–23.
- Delcourt, H.R. and Delcourt, P.A. 2000: Deciduous forests. In Barbour, M.G. and Billings, W.D., editors, *North American terrestrial vegetation* (second edition), Cambridge: Cambridge University Press, 357–95.
- Delcourt, P.A., Delcourt, H.R. and Webb, T. III 1984: *Atlas of mapped distributions of dominance and modern pollen percentages for important tree taxa of eastern North America*. Dallas: American Association of Stratigraphic Palynologists Foundation, 131 pp.
- Eidenshink, J.C. 1992: The 1990 conterminous U.S. AVHRR data set. *Photogrammetric Engineering and Remote Sensing* 58, 809–13.
- Eidenshink, J.C. and Faundeen, J.L. 1994: The 1 km AVHRR global

- land data set: first stages in implementation. *International Journal of Remote Sensing* 15, 3443–62.
- Fassnacht, K.S., Gower, S.T., MacKenzie, M.D., Nordheim, E.V. and Lillesand, T.M. 1997: Estimating the leaf area index of north central Wisconsin forests using the Landsat Thematic Mapper. *Remote Sensing of the Environment* 61, 229–45.
- Field, C.B., Randerson, J.T. and Malmström, C.M. 1995: Global net primary production: combining ecology and remote sensing. *Remote Sensing of the Environment* 51, 74–88.
- Gajewski, K., Vance, R., Sawada, M., Fung, I., Gignac, L.D., Halsey, L., John, J., Maisongrande, P., Mandell, P., Mudie, P.J., Richard, P.J.H., Sherin, A.G., Soroko, J. and Vitt, D.H. 2000: The climate of North America and adjacent ocean waters ca. 6ka. *Canadian Journal of Earth Sciences* 37, 661–81.
- Goward, S.N. and Dye, D.G. 1987: Evaluating North American net primary productivity with satellite observations. *Advances in Space Research* 7, 165–74.
- Goward, S.N., Tucker, C.J. and Dye, D.G. 1985: North American vegetation patterns observed with the NOAA-7 advanced very high resolution radiometer. *Vegetatio* 64, 3–14.
- Graulich, L.J. and Davis, M.B. 1993: Holocene variation in spatial scales of vegetation pattern in the upper Great Lakes. *Ecology* 74, 826–39.
- Guiot, J., Harrison, S.P. and Prentice, I.C. 1993: Reconstruction of Holocene precipitation patterns in Europe using pollen and lake-level data. *Quaternary Research* 40, 139–49.
- Hooghiemstra, H. 1984: *Vegetational and climatic history of the high plain of Bogota, Colombia: a continuous record of the last 3.5 million years*. Vaduz: A.R. Gantner Verlag Kommanditgesellschaft, 368 pp.
- Hunt, E.R. Jr, Piper, S.C., Nemani, R., Keeling, C.D., Otto, R.D. and Running, S.W. 1996: Global net carbon storage exchange and intrannual atmospheric CO₂ concentrations predicted by an ecosystem process model and three-dimensional atmospheric transport model. *Global Biogeochemical Cycles* 10, 431–56.
- Imbrie, J. and Kipp, N.G. 1971: A new micropaleontological method for quantitative paleoclimatology: application to a late Pleistocene Caribbean core. In Turekian, K., editor, *The late Cenozoic glacial ages*, New Haven, CT: Yale University Press, 71–181.
- Jackson, S.T. 1990: Pollen source area and representation in small lakes of the northeastern United States. *Review of Palaeobotany and Palynology* 63, 53–76.
- 1991: Pollen representation of vegetational patterns along an elevational gradient. *Journal of Vegetation Science* 2, 613–24.
- Jackson, S.T. and Kearsley, J.B. 1998: Quantitative representation of local forest composition in forest-floor pollen assemblages. *Journal of Ecology* 86, 474–90.
- Jackson, S.T. and Lyford, M.E. 1999: Pollen dispersal models in Quaternary plant ecology: assumptions, parameters, and prescriptions. *The Botanical Review* 65, 39–75.
- Jackson, S.T. and Overpeck, J.T. 2000: Responses of plant populations and communities to environmental changes of the late Quaternary. *Paleobiology* 26, 194–220.
- Jackson, S.T. and Wong, A. 1994: Using forest patchiness to determine pollen source areas of closed-canopy pollen assemblages. *Journal of Ecology* 82, 89–99.
- Jacobson, G.L. Jr, Webb, T. III and Grimm, E.C. 1987: Patterns and rates of vegetation change during the deglaciation of eastern North America. In Ruddiman, W.F. and Wright, H.E. Jr, editors, *North America and adjacent oceans during the last deglaciation*, Boulder, CO: Geological Society of America, 277–88.
- Kohfeld, K.E. and Harrison, S.P. 2000: How well can we simulate past climates? Evaluating the models using global palaeoenvironmental datasets. *Quaternary Science Reviews* 19, 321–46.
- Levis, S., Foley, J. and Pollard, D. 1999: CO₂ climate, and vegetation feedbacks at the Last Glacial Maximum. *Journal of Geophysical Research* V104(ND24), 31 191–98.
- Loveland, T.R., Reed, B.C., Brown, J.F., Ohlen, D.O., Zhu, J., Yang, L. and Merchant, J.W. 2000: Development of a global land cover characteristics database and IGBP DISCover from 1-km AVHRR data. *International Journal of Remote Sensing* 21, 1303–30.
- Nemani, R.R. and Running, S.W. 1995: Satellite monitoring of global land cover changes and their impact on climate. *Climate Change* 31, 395–413.
- 1996: Global vegetation cover changes from coarse resolution satellite data. *Journal of Geophysical Research* 101, 7145–62.
- Overpeck, J.T., Webb, T. III and Prentice, I.C. 1985: Quantitative interpretation of fossil pollen spectra: dissimilarity coefficients and the method of modern analogs. *Quaternary Research* 23, 87–108.
- Overpeck, J.T., Webb, R.S. and Webb, T. III 1992: Mapping eastern North American vegetation change of the past 18 ka: No-analogs and the future. *Geology* 20, 1071–74.
- Payette, S. 1992: Fire as a controlling process in the North American boreal forest. In Shugart, H.H., Leemans, R. and Bonan, G.B., editors, *A systems analysis of the global boreal forest*, Cambridge: Cambridge University Press, 145–69.
- Peyron, O., Guiot, J., Cheddadi, R., Tarasov, P., Reille, M., de Beaulieu, J.-L., Bottema, S. and Andrieu, V. 1998: Climatic reconstruction in Europe for 18,000 yr B.P. from pollen data. *Quaternary Research* 49, 183–96.
- Prentice, I.C. 1980: Multidimensional scaling as a research tool in Quaternary palynology: a review of theory and methods. *Review of Palaeobotany and Palynology* 31, 71–104.
- 1985: Pollen representation, source area, and basin size: toward a unified theory of pollen analysis. *Quaternary Research* 23, 76–86.
- 1988: Records of vegetation in time and space: the principles of pollen analysis. In Huntley, B. and Webb, T. III, editors, *Vegetation history*, Dordrecht: Kluwer, 17–42.
- Prentice, I.C. and Webb, T. III 1986: Pollen percentages, tree abundances and the Fagerlinde effect. *Journal of Quaternary Science* 1, 35–43.
- 1998: BIOME 6000: reconstructing global mid-Holocene vegetation patterns from palaeoecological records. *Journal of Biogeography* 25, 997–1005.
- Prentice, I.C., Bartlein, P.J. and Webb, T. III 1991: Vegetation and climate changes in eastern North America since the last glacial maximum: a response to continuous climatic forcing. *Ecology* 72, 2038–56.
- Prentice, I.C., Berglund, B.E. and Olsson, T. 1987: Quantitative forest-composition sensing characteristics of pollen samples from Swedish lakes. *Boreas* 16, 43–54.
- Prentice, I.C., Harrison, S.P., Jolly, D. and Guiot, J. 1998: The climate and biomes of Europe at 6000 yr. BP: comparison of model simulations and pollen-based reconstructions. *Quaternary Science Reviews* 17, 659–68.
- Prentice, I.C., Jolly, D. and BIOME 6000 participants 2000: Mid-Holocene and glacial-maximum vegetation geography of the northern continents and Africa. *Journal of Biogeography* 27, 507–19.
- Ramankutty, N. and Foley, J.A. 1998: Characterizing patterns of global land use: an analysis of global croplands data. *Global Biogeochemical Cycles* 12, 667–85.
- 1999a: Estimating historical changes in global land cover: croplands from 1700 to 1992. *Global Biogeochemical Cycles* 13, 997–1027.
- 1999b: Estimating historical changes in land cover: North American croplands from 1850 to 1992. *Global Ecology and Biogeography* 8, 381–96.
- Roughgarden, J., Running, S.W. and Matson, P.A. 1991: What does remote sensing do for ecology? *Ecology* 72, 1918–22.
- Rowe, J.S. 1972: *Forest regions of Canada*. Ottawa: Canadian Forestry Service, Department of Fisheries and the Environment, Publication no. 1300.
- Sugita, S. 1994: Pollen representation of vegetation in Quaternary sediments: theory and method in patchy vegetation. *Journal of Ecology* 82, 881–97.
- Sugita, S., Gaillard, M.-J. and Broström, A. 1999: Landscape openness and pollen records: a simulation approach. *The Holocene* 9, 409–21.
- Tarasov, P.E., Webb, T. III, Andreev, A.A., Afans'eva, N.B., Berezina, N.A., Bezusko, L.G., Blyakharachuk, T.A., Bolikhovskaya, N.S., Cheddadi, R., Chernavskaya, M.M., Chernova, G.M., Dorofeyev, N.I., Dirksen, V.G., Elina, G.A., Filimonova, L.V., Glebov, F.Z., Guiot, J., Gunova, V.S., Harrison, S.P., Jolly, D., Khomutova, V.I., Kvavadze, E.V., Osipova, I.M., Panova, N.K., Prentice, I.C., Saarse, L., Sevastyanov, D.V., Volkova, V.S. and Zernitskaya, V.P. 1998: Present-day and mid-Holocene biomes reconstructed from pollen and plant macrofossil data from the Former Soviet Union and Mongolia. *Journal of Biogeography* 25, 1029–53.
- Tucker, C.J., Vanpraet, C.L., Sharman, M.J. and Van Ittersum, G. 1985: Satellite remote sensing of total herbaceous biomass production in

- the Senegalese Sahel: 1980–1984. *Remote Sensing of the Environment* 17, 233–49.
- Tzedakis, P.C.** 1993: Long-term tree populations in northeast Greece through multiple Quaternary climatic cycles. *Nature* 364, 437–40.
- van Leeuwen, W.J.D., Huete, A.R., Walthall, C.L., Prince, S.D., Bégué, A. and Roujean, J.L.** 1997: Deconvolution of remotely sensed spectral mixtures for retrieval of LAI, fAPAR and soil brightness. *Journal of Hydrology* 188–189, 697–724.
- Webb, R.S. and Webb, T. III** 1988: Rates of sediment accumulation in pollen cores from small lakes and mires of eastern North America. *Quaternary Research* 30, 284–97.
- Webb, T. III** 1974: Corresponding patterns of pollen and vegetation in lower Michigan: a comparison of quantitative data. *Ecology* 55, 17–28.
- 1981: The past 11,000 years of vegetational change in eastern North America. *Bioscience* 31, 501–506.
- 1993: Constructing the past from late-Quaternary pollen data: temporal resolution and a zoom lens space-time perspective. In Kidwell, S.M. and Behrensmeier, A.K., editors, *Taphonomic approaches to time resolution in fossil assemblages*, Knoxville, TN: Paleontological Society, 79–101.
- Webb, T. III, Anderson, K.H., Bartlein, P.J. and Webb, R.S.** 1998: Late Quaternary climate change in eastern North America: a comparison of pollen-derived estimates with climate model results. *Quaternary Science Reviews* 17, 587–606.
- Webb, T. III, Bartlein, P.J., Harrison, S.P. and Anderson, K.H.** 1993: Vegetation, lake levels, and climate in eastern North America for the past 18,000 years. In Wright, H.E. Jr, Kutzbach, J.E., Webb, T. III, Ruddiman, W.F., Street-Perrott, F.A. and Bartlein, P.J., editors, *Global climates since the last glacial maximum*, Minneapolis, MN: University of Minnesota Press, 415–67.
- Webb, T. III and McAndrews, J.H.** 1976: Corresponding patterns of contemporary pollen and vegetation in central North America. *Geological Society of America Memoir* 145, 267–99.
- Webb, T. III, Richard, P.J.H. and Mott, R.J.** 1983: A mapped history of Holocene vegetation in southern Quebec. *Syllogeus* 49, 273–336.
- Williams, J.W.** 2000: *Biome-scale vegetation dynamics in North America since the last glacial maximum: maps and reconstructions from fossil pollen data and the testing of biogeography models*. PhD dissertation, Brown University, Providence, RI, 265 pp.
- 2003: Needleleaved and broadleaved tree cover distributions in North America since the last glacial maximum. *Global and Planetary Change* 35, 1–23.
- Williams, J.W., Shuman, B.N. and Webb, T. III** 2001: Dissimilarity analyses of late-Quaternary vegetation and climate in eastern North America. *Ecology* 82, 3346–62.
- Williams, J.W., Webb, T. III, Richard, P.J.H. and Newby, P.** 2000: Late Quaternary biomes of Canada and the Eastern United States. *Journal of Biogeography* 27, 585–607.
- Yu, G., Chen, X., Ni, J., Cheddadi, R., Guiot, J., Han, H., Harrison, S.P., Huang, C., Ke, M., Kong, Z., Li, S., Li, W., Liew, P., Liu, G., Liu, J., Liu, Q., Liu, K.-B., Prentice, I.C., Qui, W., Ren, G., Song, C., Sugita, S., Sun, X., Tang, L., Van Campo, E., Xia, Y., Xu, Q., Yan, S., Yang, X., Zhao, J. and Zheng, Z.** 2000: Palaeovegetation of China: a pollen data-based synthesis for the mid-Holocene and last glacial maximum. *Journal of Biogeography* 27, 635–64.